Nonlinear Vibration Analysis of Membrane SAR Antenna Structure Adopting a Vector Form Intrinsic Finite Element

Article *in* JOURNAL OF MECHANICS · June 2015

DOI: 10.1017/jmech.2014.97

CITATIONS
3

READS
137

4 authors, including:

Rui Xu
National University of Defense Technology
15 PUBLICATIONS **50** CITATIONS
SEE PROFILE

Jianping Jiang
National University of Defense Technology
19 PUBLICATIONS **115** CITATIONS
SEE PROFILE

Wang Liu
National University of Defense Technology
15 PUBLICATIONS **73** CITATIONS
SEE PROFILE

Nonlinear Vibration Analysis of Membrane SAR Antenna Structure Adopting a Vector Form Intrinsic Finite Element

R. Xu, D.-X. Li, J.-P. Jiang and W. Liu

Journal of Mechanics / *FirstView* Article / May 2015, pp 1 - 9
DOI: 10.1017/jmech.2014.97, Published online: 23 January 2015

NONLINEAR VIBRATION ANALYSIS OF MEMBRANE SAR ANTENNA STRUCTURE ADOPTING A VECTOR FORM INTRINSIC FINITE ELEMENT

R. Xu, D.-X. Li* J.-P. Jiang, W. Liu

National University of Defense Technology
Hunan, China

ABSTRACT

This study adopted the Vector Form Intrinsic Finite Element (VFIFE) method to study the nonlinear vibration of the membrane SAR (Synthetic Aperture Radar) antenna structure. As the dynamic characteristic of the antenna is mainly determined by the support frame, it can be simplified as an axially loaded cantilever beam. The linear and geometrically nonlinear models of the axially loaded cantilever beam are established. The beam is modeled as discrete mass points which are connected by deformable elements through VFIFE method. A statics analysis is first presented to verify the VFIFE method. Then effects of the geometrical nonlinearity and axial load are investigated. It is believed that the presented study is valuable for better understanding the influences of the geometrical nonlinearity and axial load of the cantilever beam on the structural vibration characteristics.

Keywords: Vector form intrinsic finite element, Membrane SAR antenna, Axially loaded beam, Nonlinear vibration.

1. INTRODUCTION

The lightweight and flexible beam structures are extensively used in aerospace engineering, civil and mechanical engineering in recent decades. Most of these beams are working under axial load. Earlier studies have shown that the axial load has more pronounced effect on the natural frequencies and mode shapes than the shear deformation and rotary inertia [1]. It is well known that a tensile axial load will increase the natural frequencies, whereas a compressive axial load decreases the natural frequencies of beams [2]. Vo *et al*. [1-3] studied the free vibration of axially loaded thin-walled composite box beams. Li *et al*. [4] researched free vibration analyses of axially loaded laminated composite beams based on higher-order shear deformation theory. Li [5] investigated the free vibration of axially loaded shear beams carrying lumped masses at elastically supported ends where rotational motion of the cross section is taken into account. Calio [6] analyzed the free vibration and the stability of axially loaded Timoshenko beams on elastic foundation through the dynamic stiffness matrix method.

For large flexible beams, the vibrations once introduced in the structure can grow up to large amplitudes [7]. The effects of geometrical nonlinearity become prominent for the dynamic behavior of beams and it is relevant to treat its impacts [8]. Some researchers had afforded their best to model and investigate it using analytical and numerical techniques. Azrar *et al*. [9,10] present a semi-analytical approach studied to the nonlinear dynamic response problem of Simply-Supported (S-S) and Clamped-Clamped (C-C) beams at large amplitudes. Jacques *et al*. [11] deals with geometrical nonlinear vibrations of sandwich beams with viscoelastic materials. Hemmatnezhad *et al*. [12] investigated the large amplitude free vibration of functionally graded beams by a finite element formulation. Mahmoodi *et al*. [13] present an experimental investigation of nonlinear vibration and frequency response analysis of cantilever viscoelastic beams.

However, only few papers investigated the dynamic behavior of axially loaded beams taking into account geometrical nonlinearities so far. Bayat *et al*. [14] used Hamilton Approach (HA) to analyze the nonlinear free vibration of S-S and for the C-C Euler-Bernoulli beams fixed at one end subjected to the axial loads.

In the present paper, the vector formed intrinsic finite element (VFIFE) method, a new computational method developed by Ting *et al*. [15,16] and Shih *et al*. [17], is adopted to solve the nonlinear vibration problem of the axially loaded cantilever beam. The basic idea of VFIFE method is to discretize the structural system into particles based on Newton's law. This method is very effective in processing large deformation problem, since it does not need structural stiffness matrix and iterative method. Wang *et al*. applied the VFIFE method to analyze nonlinear dynamic behaviors of 3D reticulated structure [18] and building system [19]. Wu *et al*. adopted the VFIFE method to do large deflection analysis for flexible frame structures [20,21] and 3D membrane structures [22,23]. Lien *et al*. applied

* Corresponding author (dongxuli@nudt.edu.cn)

DOI : 10.1017/jmech.2014.97

the VFIFE method to investigate the nonlinear behavior of steel structures exposed to fire [24,25] and the inelastic large deflection behavior for steel frames with semi-rigid joints [26]. Recently, Wu implemented the VFIFE method to perform dynamic nonlinear analysis of shell structures [27].

Compared with some previous investigations of nonlinear vibration of axially loaded beam, the major originalities and the contributions of the present work are list as follows: The influences of the geometrical nonlinearity and axial load of the cantilever beam are both taken into account, while the other papers did not study their relationship with the frequency of the beam. The VFIFE method was introduced to solve the dynamic problem of the vibrating beam, it is simpler than traditional finite element method (FEM). Plenty of numeric analysis and comparison are presented. The relationship between the frequency of the beam, the axial loads and vibration amplitude are discovered from the results.

This paper is organized as follows. First, the problem is formulated in Section 2, the linear and nonlinear governing equations are presented. Then, the VFIFE method is introduced in Section 3. Section 4 presents the numerical results of different load and different amplitude. Finally, conclusion are made in Section 5.

2. PROBLEM FORMULATION

A membrane SAR (Synthetic Aperture Radar) antenna is considered in this paper. It is typically composed of four components, a support frame, a membrane, tension cables and floating steadying bars as shown in Fig. 1. The function of support frame and floating steading bars are produce a constant tension for the membrane. Hence, they are in axially loaded state. As the membrane and the floating steadying bars are rather light weighted, the first order frequency of the membrane SAR antenna is rather decided by the support frame. Moreover, the frame can be simplified as a cantilever beam with length L, a cross section area S, a moment of inertia I, a density ρ and a modulus of elastic E, which is axially compressed by a loading N as shown in Fig. 2. Denoting by u and w are the axial and transverse deflection, respectively.

2.1 Linear Model of Axial Loaded Beam

Considering axial load, the free vibration of then beam becomes:

$$EI\frac{\mathrm{d}^4 w}{\mathrm{d}x^4}+N\frac{\partial^2 w}{\partial x^2}+\rho S\frac{\partial^2 w}{\partial t^2}=0 \tag{1}$$

Suppose the transverse deflection curve of the beam is $w(x, t)$, adopting method of separation of variables, assume:

$$w=X(x)\cdot Y(t) \tag{2}$$

Equation (1) can be written as:

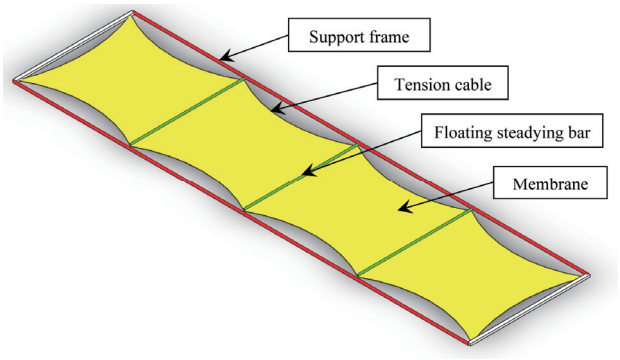

Fig.1 The membrane SAR antenna.

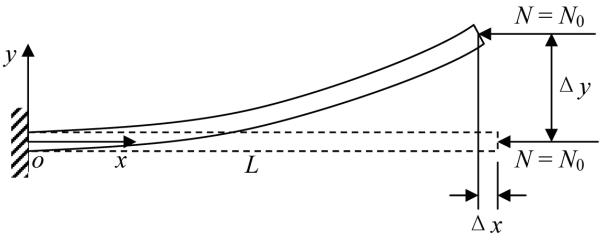

Fig. 2 The axially loaded cantilever beam.

$$EI\frac{X''''}{X}+N\frac{X''}{X}=-\rho S\frac{\ddot{Y}(t)}{Y(t)}=\text{const} \tag{3}$$

Then

$$\ddot{Y}(t)+\omega^2 Y(t)=0 \tag{4}$$

and

$$EI\cdot X''''(x)+NX''(x)-\rho S\omega^2 X(x)=0 \tag{5}$$

From Eq. (4) we can get

$$Y(t)=\alpha\sin\omega t+\beta\cos\omega t \tag{6}$$

It illustrates that the free vibration of the axial loaded beam is still simple harmonic vibration, the circular frequency is ω.

Equation (5) can be simplified as:

$$X''''(x)+g^2X''(x)-a^4X(x)=0 \tag{7}$$

where

$$a^4=\frac{\rho S\omega^2}{EI} \tag{8}$$

$$g^2=\frac{N}{EI}=\frac{N}{N_{cr}}\frac{N_{cr}}{EI} \tag{9}$$

where N_{cr} is the critical load of the beam, for the cantilever beam considered in this paper $N_{cr}=\pi^2EI/4L^2$.

The characteristic equation of Eq. (7) is:

$$r^4+g^2r^2-a^4=0 \tag{10}$$

then

$$r = \pm i\delta \quad \text{and} \quad \pm\varepsilon \tag{11}$$

The general solution of Eq. (7) is

$$X(x) = A\sin\delta x + B\cos\delta x + C\mathrm{sh}\varepsilon x + D\mathrm{ch}\varepsilon x \tag{12}$$

where

$$\delta = \sqrt{\left(a^4 + \frac{g^4}{4}\right)^{\frac{1}{2}} + \frac{1}{2}g^2} \tag{13}$$

$$\varepsilon = \sqrt{\left(a^4 + \frac{g^4}{4}\right)^{\frac{1}{2}} - \frac{1}{2}g^2} \tag{14}$$

and the constant of integration A、B、C、D are determined by the boundary conditions.

For cantilever beam, the boundary conditions are:

$$\begin{aligned} &X(0) = 0, && X'(0) = 0 \\ &X''(L) = 0, && EI \cdot X'''(L) = -N \cdot X'(L) \end{aligned} \tag{15}$$

From the boundary conditions, we can get

$$2\delta^2\varepsilon^2 - \delta\varepsilon g^2 \sin\delta L\,\mathrm{sh}\,\varepsilon L + (\varepsilon^4 + \delta^4)\cos\delta L\,\mathrm{ch}\,\varepsilon L = 0 \tag{16}$$

For given N/N_{cr}, the vibration frequency can be solved by Eq. (16).

2.2 Geometrical Nonlinear Model of Axial Loaded Beam

Equation (1) is based on small deformation theory. But while the beam is in large-amplitude vibrating, the small deformation theory will be not valid. According to von Karman's theory, the kinematics' relation for such beams are:

$$\varepsilon_{xx} = \frac{\partial u}{\partial x} + \frac{1}{2}\left(\frac{\partial w}{\partial x}\right)^2 - y\frac{\partial^2 w}{\partial x^2} \tag{17}$$

where ε_{xx} is the longitudinal (or normal) strain, $u = u(x, t)$ and $w = w(x, t)$ represent the displacements of an arbitrary point located on the beam's neutral axis in the x and y directions, respectively.

By applying Hamilton's principle, the nonlinear governing coupled PDEs of motion for the problem at hand are as follows:

Force relation in x direction:

$$\rho S\frac{\partial^2 u}{\partial t^2} - ES\frac{\partial}{\partial x}\left[\frac{\partial u}{\partial x} - \frac{\partial u}{\partial x}\left(\frac{\partial w}{\partial x}\right)^2 + \frac{1}{2}\left(\frac{\partial w}{\partial x}\right)^2\right] = N \tag{18}$$

Force relation in y direction:

$$\begin{aligned} &\rho S\frac{\partial^2 w}{\partial t^2} + EI\frac{\partial^4 w}{\partial x^4} + N\frac{\partial^2 w}{\partial t^2} \\ &\quad - ES\frac{\partial}{\partial x}\left\{\frac{\partial w}{\partial x}\left[\frac{\partial u}{\partial x} + \frac{1}{2}\left(\frac{\partial w}{\partial x}\right)^2 - \left(\frac{\partial u}{\partial x}\right)^2\right]\right\} = 0 \end{aligned} \tag{19}$$

where u and w are the axial and bending displacement, respectively.

3. VECTOR FORM INTRINSIC FINITE ELEMENT METHOD

3.1 Basic Assumptions

The basic modeling assumptions of VFIFE are essentially the same as those for the classical structural. A lumped-mass idealization is first performed to construct a discrete model of a continuous structure. For the cantilever beam considered in this paper, it is modeled as a system of discrete mass points, shown in Fig. 3. All these mass point are then connected by deformable elements without mass and are in equilibrium. Then the structural geometry is defined by the trajectories of connection masses.

Assume that the motion of each individual node (mass point) follows Newton's law, the equations of motion for node i at time t are written as

$$\boldsymbol{M}_i\ddot{\boldsymbol{d}}_i(t) = \boldsymbol{F}_i^{ext}(t) - \boldsymbol{F}_i^{\mathrm{int}}(t) \tag{20}$$

where $\boldsymbol{M}_i = \mathrm{diag}(m_i, m_i, I_i)$ is the diagonal mass matrix of the node i, m_i and I_i are the mass and moment of inertia of the node; $\boldsymbol{d}_i(t)$ is the displacement vector; $\boldsymbol{F}_i^{ext}(t)$ is the vector of applied forces or equivalent forces acting on the node, $\boldsymbol{F}_i^{\mathrm{int}}(t)$ is the vector of total resistance forces or internal resultant forces by all the elements connecting with this node.

3.2 Deformation Coordinates

To calculate the deformation and internal stresses of an element, assuming the initial position at time t_0 is (1_0, 2_0); the position at time $t_a = t - \tau$ is (1_a, 2_a), and the current position at time t is (1, 2), as shown in Fig. 4. The displacement of the element from initial time t_0 to reference time t_a is ($\mathbf{u}_{1a}$, $\mathbf{u}_{2a}$), the displacement at the present time t is ($\mathbf{u}_1$, $\mathbf{u}_2$) = ($\mathbf{u}_{1a} + \Delta\mathbf{u}_1$, $\mathbf{u}_{2a} + \Delta\mathbf{u}_2$).

In order to deduction the rigid body translation and rotations from deformation increments, take node 1_a as the origin of the deformation coordinates and the x axis passes through node 2_a, as shown in Fig. 5. Transfer node 1 to node 1_a with a displacement vector $\Delta\mathbf{u}_1$, then the relative displacements between the reference configuration and the current configuration at those node 1 and 2 are:

$$\begin{cases} \Delta\boldsymbol{\eta}_1 = 0 \\ \Delta\boldsymbol{\eta}_2 = \Delta\mathbf{u}_2 - \Delta\mathbf{u}_1 \end{cases} \tag{21}$$

Then take a fictitious reverse rotation with an angle $\Delta\theta = \arccos(\mathbf{e}_t, \mathbf{e}_a)$ ($\mathbf{e}_t$ and $\mathbf{e}_a$ are the unit vector of the element at time t and t_a, respectively), the configuration of the element (1, 2) became (1′, 2′). The relative displacement increment of deformation is

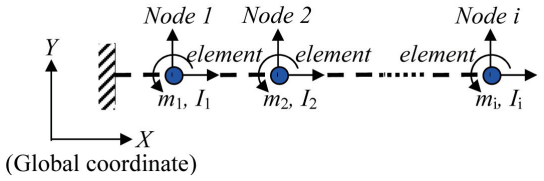

Fig. 3 The discrete model of the beam.

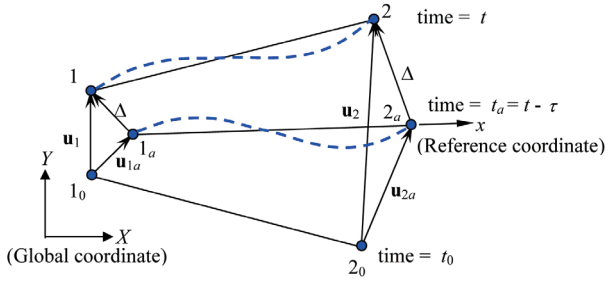

Fig. 4 Deformation coordinates for an element.

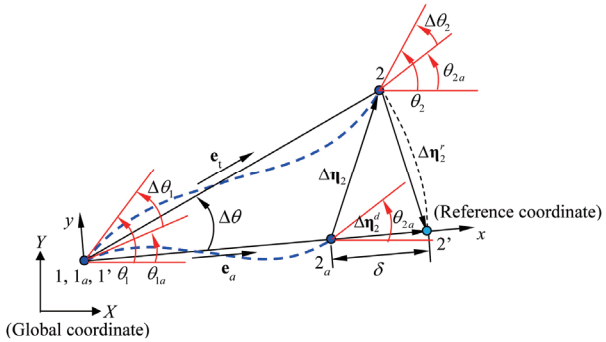

Fig. 5 Fictitious reversed rigid body motion.

$$\begin{cases}\Delta\boldsymbol{\eta}_1^d = 0 \\ \Delta\boldsymbol{\eta}_2^d = \Delta\boldsymbol{\eta}_2 - \Delta\boldsymbol{\eta}_2^r = \delta\mathbf{e}_a\end{cases} \tag{22}$$

where δ is the deformation of the element length, $\Delta\boldsymbol{\eta}_2^r$ is the rigid body displacement of node 2.

The orientation angles displacement by deduced rigid body rotations is:

$$\begin{cases}\tilde{\theta}_1 = \Delta\theta_1 - \Delta\theta = \theta_1 - \theta_{1a} - \Delta\theta \\ \tilde{\theta}_2 = \Delta\theta_2 - \Delta\theta = \theta_2 - \theta_{2a} - \Delta\theta\end{cases} \tag{23}$$

As a result, a two-node plane frame element has three independent variables δ, $\tilde{\theta}_1$ and $\tilde{\theta}_2$.

3.3 The Internal Force of the Element

For a two node frame element, the internal nodal force vector at time t is $\hat{\mathbf{f}}^{\text{int}} = \left[\hat{f}_{1x}, \hat{f}_{1y}, \hat{m}_{1z}, \hat{f}_{2x}, \hat{f}_{2y}, \hat{m}_{2z}\right]^T$, let $\hat{\mathbf{f}}^{\text{int}*} = \left[\hat{f}_{2x}, \hat{m}_{1z}, \hat{m}_{2z}\right]^T$ is the specific internal nodal force vector, it can be calculated by

$$\hat{\mathbf{f}}^{\text{int}*} = \hat{\mathbf{f}}_a^{\text{int}*} + \Delta\hat{\mathbf{f}}^{\text{int}*} \tag{24}$$

where $\hat{\mathbf{f}}_a^{\text{int}*}$ is the nodal force vector corresponding to the state of stress at time t_a, $\Delta\hat{\mathbf{f}}^{\text{int}*}$ is the incremental nodal force vector. According to the principle of virtual work, $\Delta\hat{\mathbf{f}}^{\text{int}*}$ can be calculated by

$$\Delta\hat{\mathbf{f}}^{\text{int}*} = \begin{Bmatrix}\Delta\hat{f}_{2x} \\ \Delta\hat{m}_{1z} \\ \Delta\hat{m}_{2z}\end{Bmatrix} = \frac{E_a}{l_a}\begin{bmatrix}A_a & 0 & 0 \\ 0 & 4I_a & 2I_a \\ 0 & 2I_a & 4I_a\end{bmatrix}\begin{Bmatrix}\delta \\ \tilde{\theta}_1 \\ \tilde{\theta}_2\end{Bmatrix} \tag{25}$$

From the static equilibrium equations, all the internal forces at the two nodes of the element can be calculated as:

$$\begin{cases}\sum F_x = 0 & \hat{f}_{1x} = -\hat{f}_{2x} \\ \sum M = 0 & \hat{f}_{2y} = -(\hat{m}_{1z} + \hat{m}_{2z})/l_a \\ \sum F_y = 0 & \hat{f}_{1y} = -\hat{f}_{2y}\end{cases} \tag{26}$$

The global internal nodal force vector at time t is

$$\mathbf{f}^{\text{int}} = \mathbf{T}^T\hat{\mathbf{f}}^{\text{int}} \tag{27}$$

$$\mathbf{T} = \begin{bmatrix}\mathbf{Q} & 0 & 0 & 0 \\ 0 & 1 & 0 & 0 \\ 0 & 0 & \mathbf{Q} & 0 \\ 0 & 0 & 0 & 1\end{bmatrix} \tag{28}$$

$$\mathbf{Q} = \begin{bmatrix}\cos\theta & \sin\theta \\ -\sin\theta & \cos\theta\end{bmatrix} \tag{29}$$

where θ is the orientation angle of the x axis relative to the fixed global reference coordinates.

3.4 Equation of Motion

After calculating all the internal forces of element nodes, one can sum over all internal forces $-\mathbf{F}^{int}$ and external forces $\mathbf{F}^{ext}$ on a mass point i and obtain the following equation of motion without damping effect:

$$\mathbf{M}\ddot{\mathbf{d}} = \mathbf{F}^{ext} - \mathbf{F}^{int} \tag{30}$$

where $\mathbf{M}$ is the general mass matrix and $\mathbf{d}$ is the general displacement vector.

In this paper, the explicit time integration technique is used to solve the Eq. (30).

4. NUMERICAL RESULTS AND DISCUSSIONS

4.1 Model Verification

In order to verify the accuracy and reliability of the VFIFE method, we first do statics analysis of the nonlinear cantilever beam. The length of the beam is L = 1 m, cross sectional area $S = 4 \times 10^{-6}\text{m}^2$, moment inertias are $I = 8 \times 10^{-10}\text{m}^2$, Young's modulus $E = 2.0 \times 10^{11}\text{N/m}^2$, mass density $\rho = 1 \times 10^3\text{kg/m}^3$. Suppose a concentrated force $P = K \times EI/L^2$ is applied on the end of the beam vertically, where K is the load factor. The deflection of the beam for different K is calculated by

the VFIFE method and shown in Fig. 6(a). Figure 6(b) presents the comparison of the VFIFE results with the theory one and Updated Lagrange (UL, a nonlinear finite element method widely used for large strain problem) one. It can be observed that the VFIFE results yield good agreement with those of the theory one and UL one.

4.2 The Effect of Geometrical Nonlinearity

In order to investigate the effect of geometrical nonlinearity, the simulations of free vibration of the cantilever beam under different amplitude are presented. The time history plots are shown in Fig. 7. It indicate that the geometrical nonlinearity effect almost did not change the frequency of the beam while there is no axial load. The phase plots are shown in Fig. 8. Typical quasi-periodic motion characteristics are displayed in it.

4.3 The Effect of Axial Load

For comparison purpose, the effect of axial load for linear beam model is investigated here. For any given axial load coefficient N/N_{cr}, the vibration frequency of the beam can be solved by Eq. (16). Fig. shows the relationship between axial load and the natural frequency. The load-frequency curve determined that the value of the axial load for which the natural frequency vanishes constitutes the critical load. Figure 9 also displays the variations of natural frequency square through the axial load coefficient. Obviously, negative linear relationship can be found between them, which can be described in the following equation:

$$\omega^2 = \omega_0^2\left(1-\frac{N}{N_{cr}}\right) \tag{31}$$

where $\omega_0 = \dfrac{3.516}{L^2}\sqrt{\dfrac{EI}{\rho}}$ is the natural frequency of the cantilever beam with no axial load.

4.4 The Coupled Effects

The interaction diagram between the axial load and the first natural frequencies under different amplitude is displayed in Fig. 10. Figure 11(a) ~ 11(b) present these data in the other two forms. From Fig. 10 we can find that all curves follow a similar pattern. In all these curves the frequency decreases by increasing the axial load. Figure 11(a) demonstrates the effect of axial load on the amplitude-frequency curve. If the axial load is nonzero, the greater the amplitude of vibration, the higher the frequency of the beam. The influence of amplitude on nonlinear to linear frequency base on the axial load coefficient N/N_{cr} are presented in Fig. 11(b). In this figure, the Y-axis indicates ω_L / ω_{NL}, where ω_L and ω_{NL} are the frequency of the linear model beam and the nonlinear model beam under certain axial load, respectively. And it indicates that the greater the amplitude of vibration, the higher nonlinear to linear frequency ratio. Figures 12 to 15 show the comparison of the phase curves. When the axial load increases the phase curves become flat.

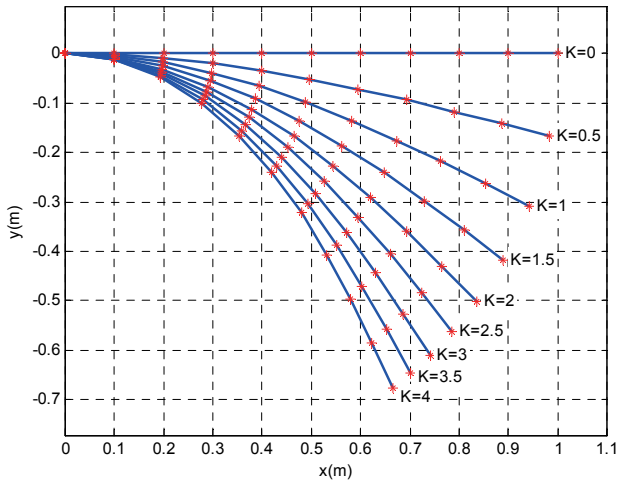

(a)

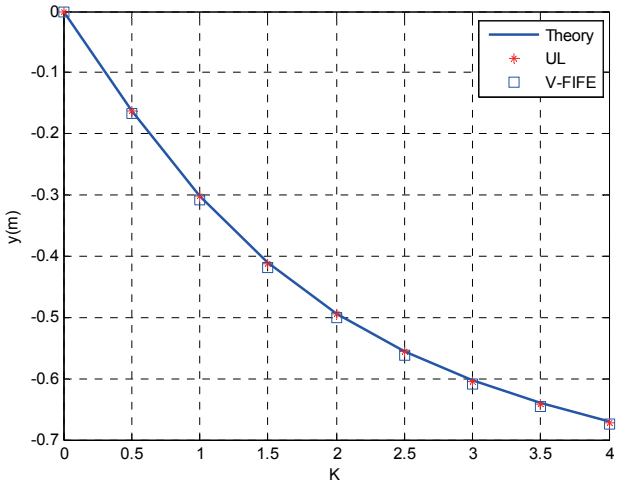

(b)

Fig. 6 Statics analysis of the nonlinear cantilever beam.

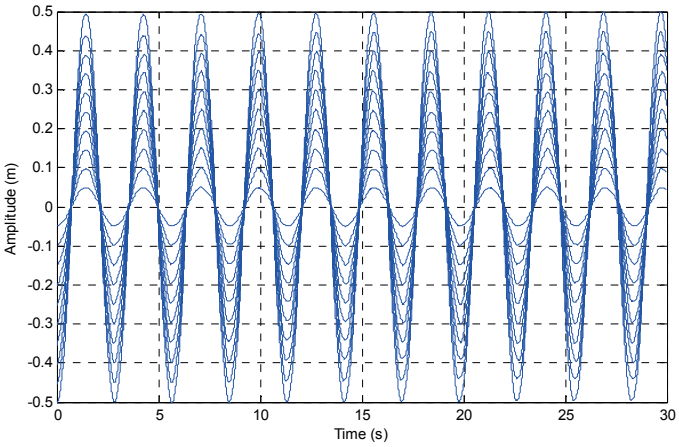

Fig. 7 Time history plots of the free vibration beam of different amplitude.

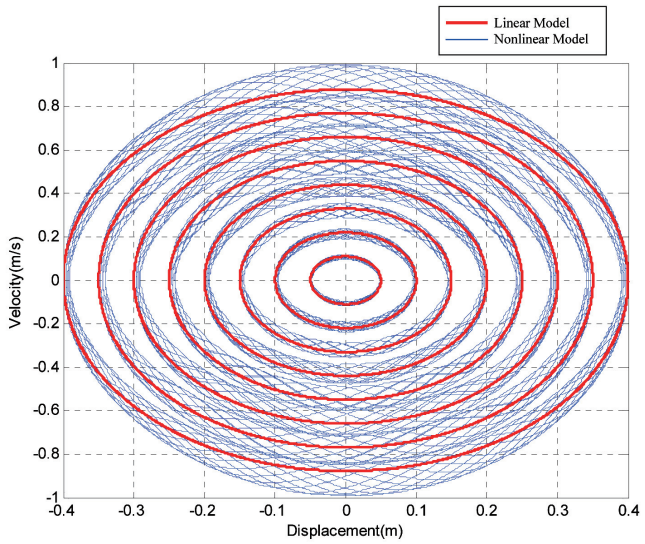

Fig. 8 Phase plots of the free vibration beam of different amplitude.

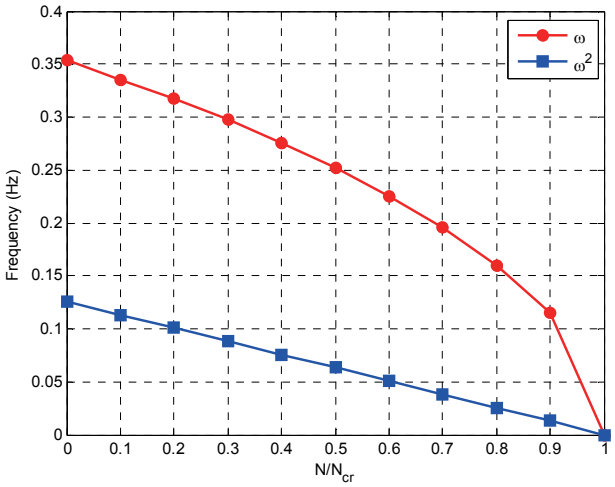

Fig. 9 Effect of axial force on the first natural frequencies.

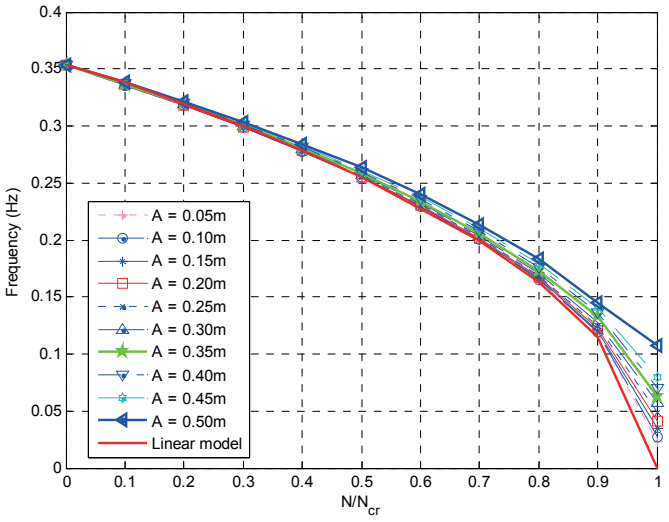

Fig. 10 Load-frequency interaction curves under different amplitude.

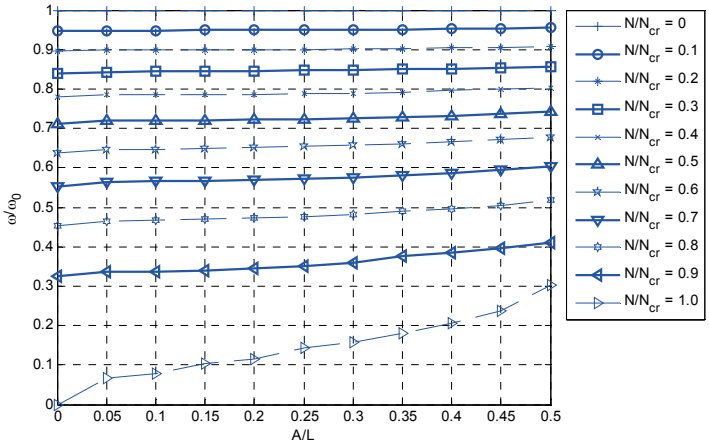

(a)

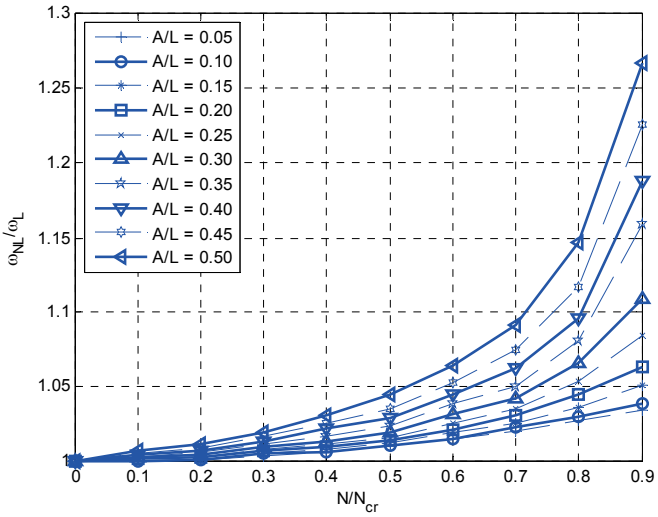

(b)

Fig. 11 Effect of geometrical nonlinearity and axial force on the first natural frequency.

5. CONCLUSIONS

The large amplitude vibration analysis of axially loaded beams is investigated numerically by means of the VFIFE method. First, the linear and geometrically nonlinear models of the axially loaded cantilever beam are established. Then the VFIFE method is introduced to solve the nonlinear problem. In order to verify the accuracy and reliability of the VFIFE method, statics analysis of the nonlinear cantilever beam are presented. Finally, the effects of geometrical nonlinearity and axial load are studied. The following conclusions can be drawn:

1. The geometrical nonlinearity effect almost did not change the frequency of the beam while there is no axial load.
2. A compressive axial load will decrease the natural frequencies of beams. For the linear model, the square of the natural frequency is negative linear dependence on the axial load.

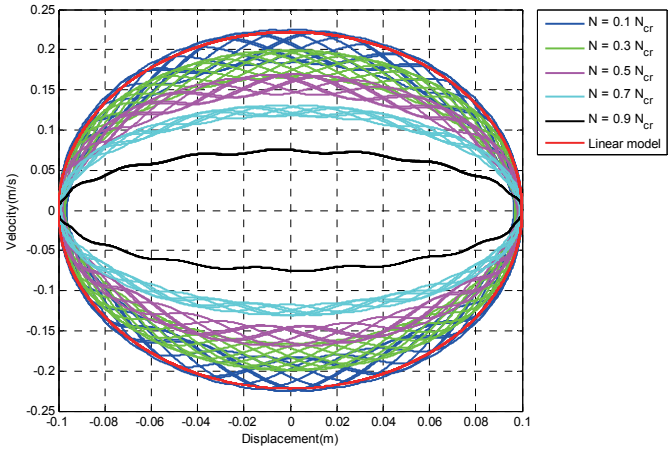

(a)

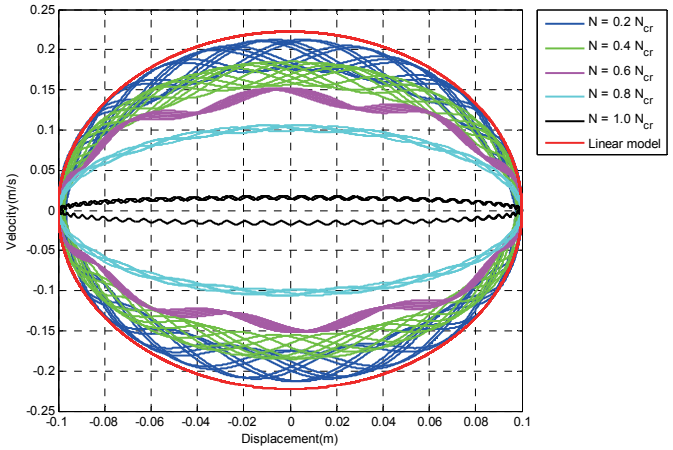

(b)

Fig. 12 Effect of axial load (A = 0.1m).

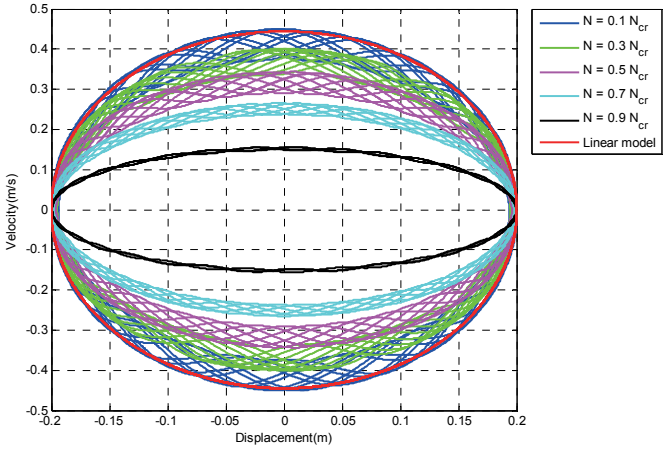

(a)

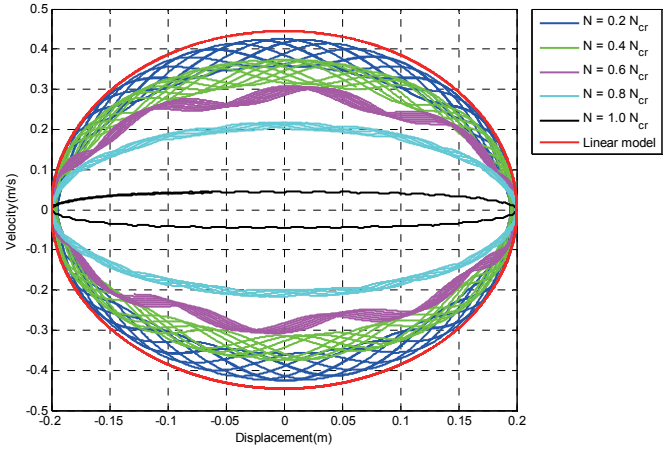

(b)

Fig. 13 Effect of axial load (A = 0.2m).

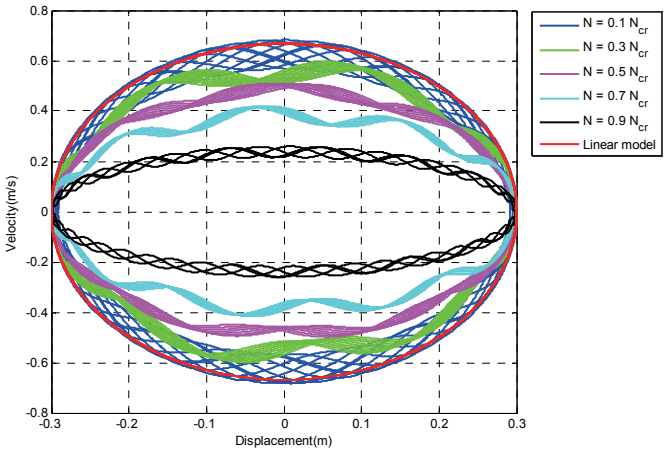

(a)

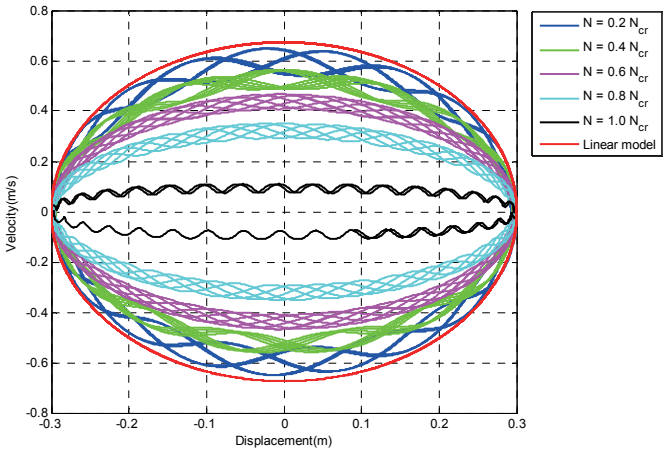

(b)

Fig. 14 Effect of axial load (A = 0.3m).

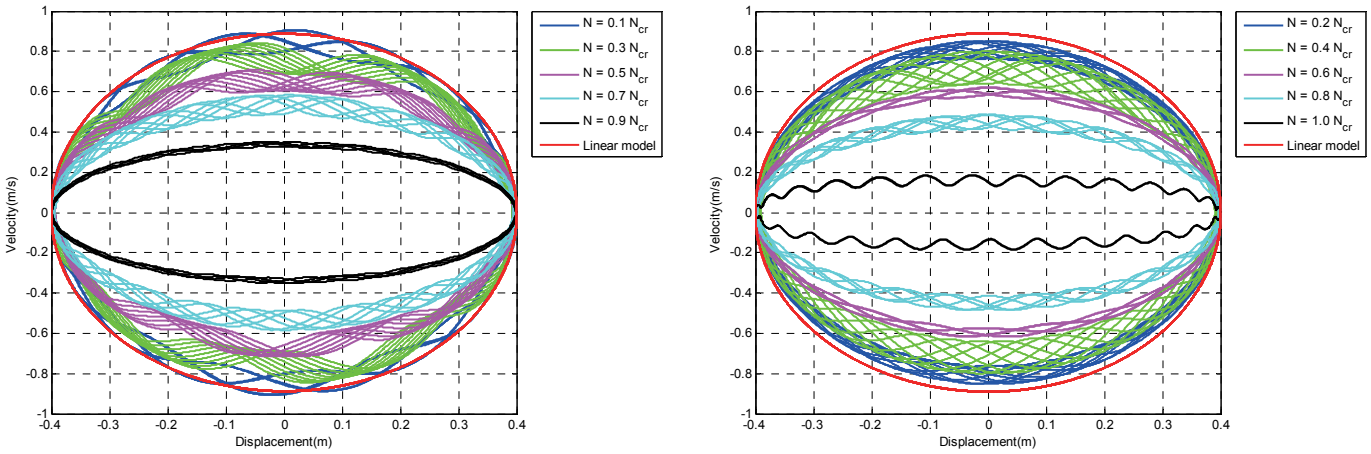

(a) (b)

Fig. 15 Effect of axial load (A = 0.4m).

3. When compressive axial load exist, the geometrical nonlinearity effect will increase the frequency of beams. And this kind of effect will be enlarged while the axial load increased.
4. The nonlinear to linear frequency ratio of the beam is increasing with the vibration amplitude.

ACKNOWLEDGEMENTS

This work was supported by the "Twelfth Five" National Defense Pre-research Program Foundation of China.

R. Xu wishes to thank Dr. Y.F. Duan of Zhejiang University for all his kindness and help.

REFERENCES

1. Vo, T. P. and Lee, J., "Free Vibration of Axially Loaded Thin-Walled Composite Box Beams," *Composite Structures*, **90**, pp. 233–241 (2009).
2. Vo, T. P. and Lee, J., "Free Vibration of Axially Loaded Thin-Walled Composite Timoshenko Beams," *Archive of Applied Mechanics*, **81**, pp. 1165–1180 (2011).
3. Vo, T. P. and Huu-Tai, T., "Free Vibration of Axially Loaded Rectangular Composite Beams Using Refined Shear Deformation Theory," *Composite Structures*, **94**, pp. 3379–3387 (2012).
4. Li, J. and Hua, H., "Free Vibration Analyses of Axially Loaded Laminated Composite Beams Based on Higher-Order Shear Deformation Theory," *Meccanica*, **46**, pp. 1299–1317 (2011).
5. Li, X. F., "Free Vibration of Axially Loaded Shear Beams Carrying Elastically Restrained Lumped Tip Masses via Asymptotic Timoshenko Beam Theory," *Journal of Engineering Mechanics*, **139**, pp. 418–428 (2013).
6. Calio, I. and Greco, A., "Free Vibrations of Timoshenko Beam Columns on Pasternak Foundations," *Journal of Vibration and Control*, **19**, pp. 686–696 (2013).
7. Belouettar, S. *et al*., "Active Control of Nonlinear Vibration of Sandwich Piezoelectric Beams: A Simplified Approach," *Computers & Structures*, **86**, pp. 386–397 (2008).
8. Azrar, L., Belouettar, S. and Wauer, J., "Nonlinear Vibration Analysis of Actively Loaded Sandwich Piezoelectric Beams with Geometric Imperfections," *Computers & Structures*, **86**, pp. 2182–2191 (2008).
9. Azrar, L., Benamar, R. and White, R. G., "A Semi-Analytical Approach to the Non-Linear Dynamics Response Problem of S-S and C-C Beams at Large Amplitudes. Part I: General Theory and Application to the Single Mode Approach to the Free and Forced Vibration Analysis," *Journal of Sound and Vibration*, **224**, pp. 183–207 (1999).
10. Azrar, L., Benamar, R. and White, R. G., "A Semi-Analytical Approach to the Non-Linear Dynamics Response Problem of S-S and C-C Beams at Large Amplitudes. Part II: Multimode Approach to the Steady State Forced Periodic Response," *Journal of Sound and Vibration*, **255**, pp. 1–41 (2002).
11. Jacques, N., Daya, E. M. and Potier-Ferry, M., "Non-Linear Vibration of Viscoelastic Sandwich Beams by the Harmonic Balance and Finite Element Methods," *Journal of Sound and Vibration*, **329**, pp. 4251–4265 (2010).
12. Hemmatnezhad, M., Ansari, R. and Rahimi, G. H., "Large-Amplitude Free Vibrations of Functionally Graded Beams by Means of a Finite Element Formulation," *Applied Mathematical Modelling*, **37**, pp. 8495–8504 (2013).
13. Mahmoodi, S. N., Jalili, N. and Khadem, S. E., "An Experimental Investigation of Nonlinear Vibration and Frequency Response Analysis of Cantilever Viscoelastic Beams," *Journal of Sound and Vibration*, **311**, pp. 1409–1419 (2008).
14. Bayat, M., Pakar, I. and Bayat, M., "On the Large Amplitude Free Vibrations of Axially Loaded Euler-Bernoulli Beams," *Steel and Composite Structures*, **14**, pp. 73–83 (2013).

15. Ting, E. C., Shih, C. and Wang, Y. K., "Fundamentals of a Vector Form Intrinsic Finite Element: Part II, Plane Solid Elements," *Journal of Mechanics*, **20**, pp. 123–132 (2004).
16. Ting, E. C., Shih, C. and Wang, Y. K., "Fundamentals of a Vector form Intrinsic Finite Element: Part I, Basic Procedure and a Plane Frame Element," *Journal of Mechanics*, **20**, pp. 113–122 (2004).
17. Shih, C., Wang, Y. K. and Ting, E. C., "Fundamentals of a Vector form Intrinsic Finite Element: Part III, Convected Material Frame and Examples," *Journal of Mechanics*, **20**, pp. 133–143 (2004).
18. Wang, C. Y. *et al*., "Nonlinear Dynamic Analysis of Reticulated Space Truss Structures," *Journal of Mechanics*, **22**, pp. 199–212 (2006).
19. Wang, C.-Y., Wang, R.-Z. and Tsai, K.-C., "Numerical Simulation of the Progressive Failure and Collapse of Structure Under Seismic and Impact Loading," *4th International Conference on Earthquake Engineering*, Taipei, Taiwan (2006).
20. Wu, T. Y., Wang, R. Z. and Wang, C. Y., "Large Deflection Analysis of Flexible Planar Frames," *Journal of the Chinese Institute of Engineers*, **29**, pp. 593–606 (2006).
21. Wu, T.-Y., Tsai, W.-C. and Lee, J.-J., "Dynamic Elastic-Plastic and Large Deflection Analyses of Frame Structures Using Motion Analysis of Structures," *Thin-Walled Structures*, **47**, pp. 1177–1190 (2009).
22. Wu, T. Y., *et al*., "Motion Analysis of 3D Membrane Structures by a Vector form Intrinsic Finite Element," *Journal of the Chinese Institute of Engineers*, **30**, pp. 961–976 (2007).
23. Wu, T. Y. and Ting, E. C., "Large Deflection Analysis of 3D Membrane Structures by a 4-Node Quadrilateral Intrinsic Element," *Thin-Walled Structures*, **46**, pp. 261–275 (2008).
24. Lien, K. H., *et al*., "Nonlinear Behavior of Steel Structures Considering the Cooling Phase of a Fire," *Journal of Constructional Steel Research*, **65**, pp. 1776–1786 (2009).
25. Lien, K. H., *et al*., "Vector form Intrinsic Finite Element Analysis of Nonlinear Behavior of Steel Structures Exposed to Fire," *Engineering Structures*, **32**, pp. 80–92 (2010).
26. Lien, K. H., Chiou, Y. J. and Hsiao, P. A., "Vector Form Intrinsic Finite-Element Analysis of Steel Frames with Semirigid Joints," *Journal of Structural Engineering*, **138**, pp. 327–336 (2012).
27. Wu, T.-Y., "Dynamic Nonlinear Analysis of Shell Structures Using a Vector form Intrinsic Finite Element," *Engineering Structures*, **56**, pp. 2028–2040 (2013).

(Manuscript received May 21, 2014,
accepted for publication September 10, 2014.)